

PHOTOMOD Radar software for Sentinel-1 data processing

Table of contents

Digital elevation model creation by the two-pass interferometry method.....	2
Creating a surface type digital map by the interferometric method.....	7
Detecting surface vessels and estimating their characteristics	12
Detecting oil slicks in radar imagery	16
Analyzing sea waves in radar imagery	20
Orthorectifying of radar imagery	23

Technical availability of free [Sentinel-1](#) radar imagery gives good opportunities for their use to solve a wide range of applied problems in the area of Earth remote sensing.

This paper illustrates some [PHOTOMOD Radar](#) software package capabilities for Sentinel-1 imagery processing. The paper comprises several processing examples.

Digital elevation model creation by the two-pass interferometry method

Below, we present two example SAR images of a terrain site in Brazil obtained by Sentinel-1 (A, B) on June 8 and 12, 2019.

Product type for both images is SLC (slant range images without non-coherent summation), Stripmap mode, and HV polarization are used.

The processing is performed in the “Interferometry” unit of the PHOTOMOD Radar (InSAR/DInSAR) software.

After the input of pre-converted into the internal PHOTOMOD Radar format images, the images are matched with subpixel accuracy.

Main operations after image matching are illustrated below using the example of an image fragment.

The values of a complex interferogram and coherence are computed. The results are given in Fig. 1.

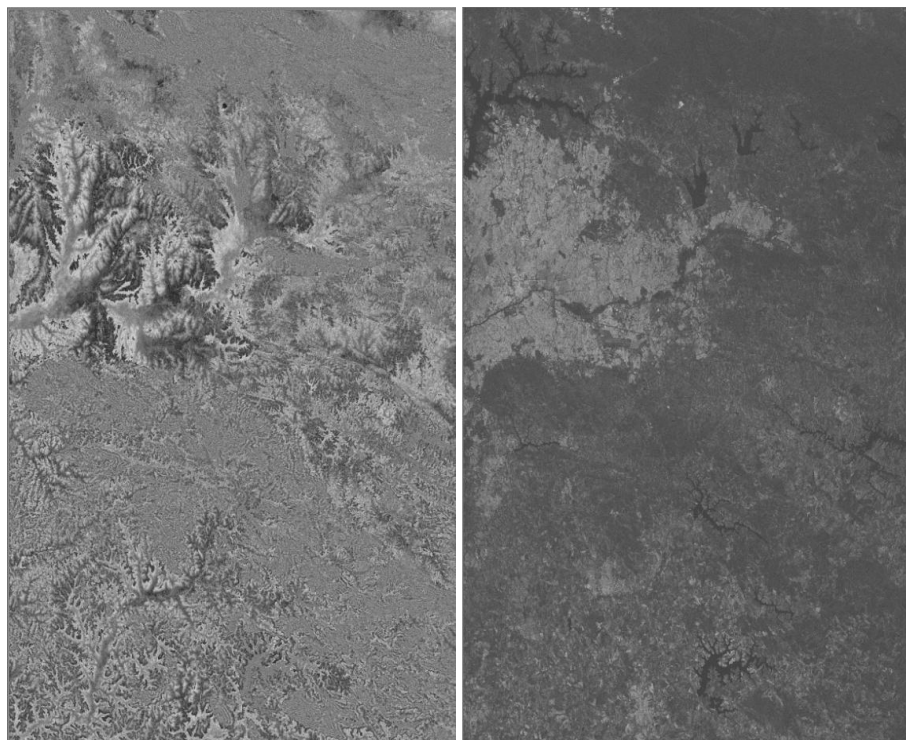


Fig. 1. Interferogram (left) and coherence (right) images

After filtering, the interferogram is as follows (Fig. 2):



Fig. 2. Interferogram filtering result.

Then, phase unwrapping is carried out, i.e. the recalculation of the relative phase (between 0 and 2π) into the absolute one, continuous at the image margin. The results are given below: the grayscale images in Fig. 3 are the result of the phase unwrapping procedure, and Fig. 4 gives a 3D unwrapped phase representation.

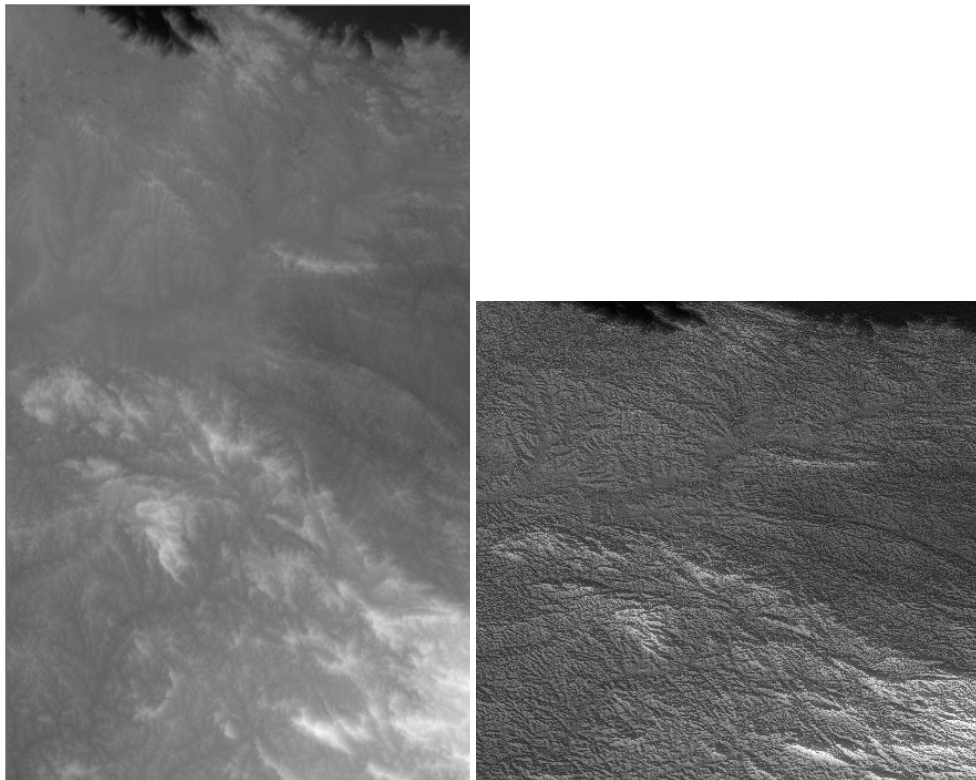


Fig. 3. Phase unwrapping result

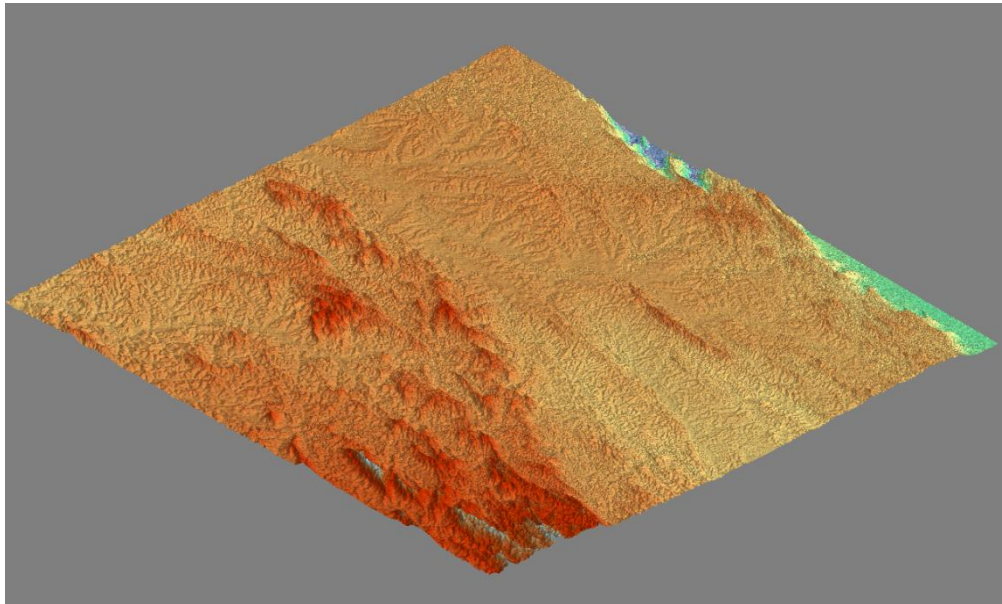


Fig. 4. Unwrapped phase 3D representation

An interface of recalculation of phase values into the absolute terrain is shown in Fig. 5. The recalculation is carried out using ground control points (GCP).

Nº	Name	Active	Color	Xm	Ym	Zm	Height	RMS error
1	GCP 1	v	Red	3020	15033	655862	223.00	0
2	GCP 2	v	Red	438	27760	21.3776	740.00	1
3	GCP 3	v	Red	9271	26639	26.2488	750.00	-6
4	GCP 4	v	Red	11267	26607	22.1359	700.00	7
5	GCP 5	v	Red	18344	23213	25	578.00	0
6	GCP 7	v	Red	18443	14858	23.0868	7.00	0
7	GCP 9	v	Red	10503	43385	36.8782	831.00	0

Fig. 5. An appearance of a dialog to collect GCPs to recalculate interferometric phase into height.

The final step is the geocoding of the resulting terrain DEM and orthorectification of one of the initial images (master file) of interferometric pair using the resulting terrain model. The results are given in Figs. 6 and 7, respectively.

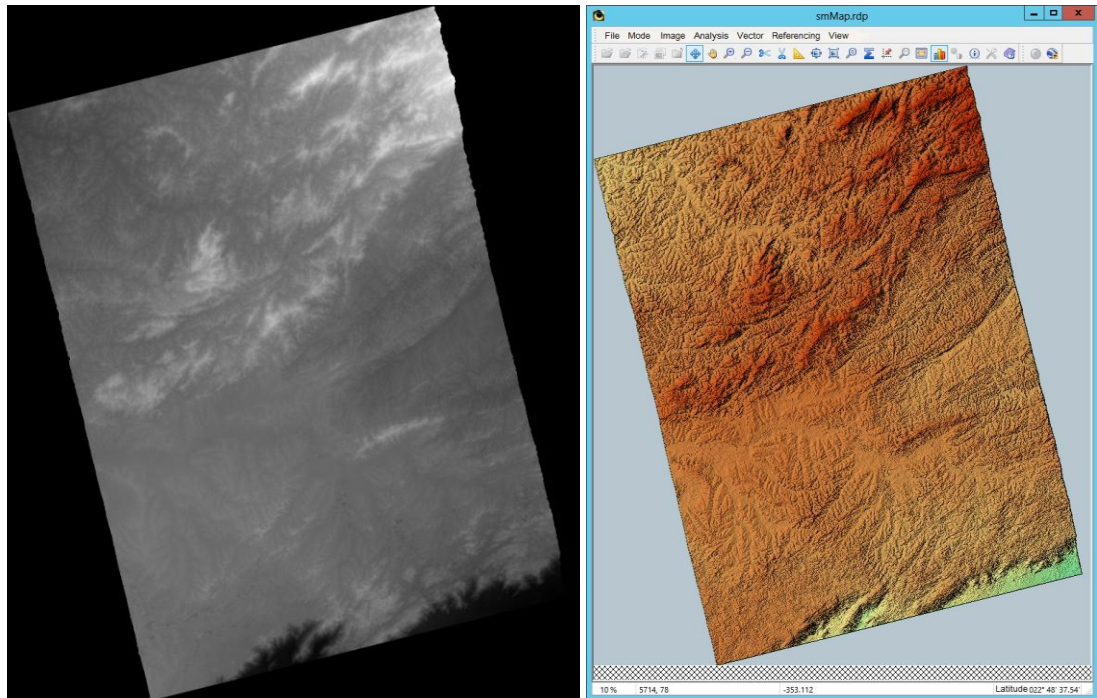


Fig. 6. The geocoding result is the digital elevation model in the geographic coordinate system

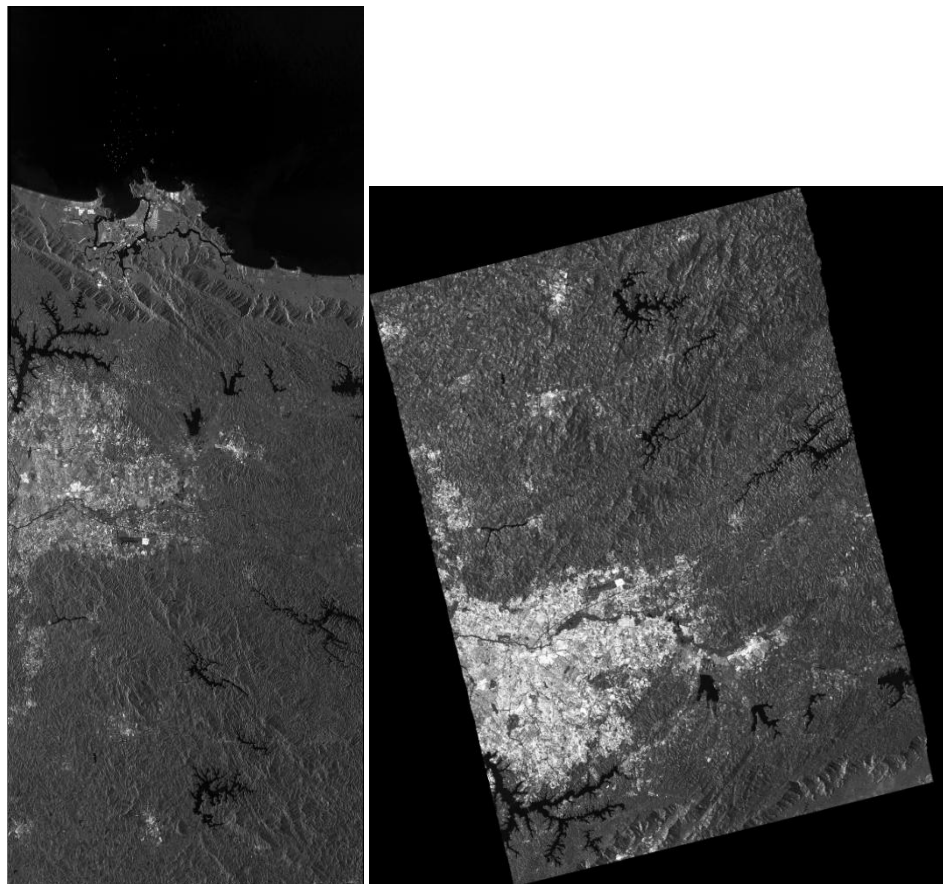


Fig. 7. A slant range image (left). A fragment of the master image orthorectified using the interferometric DTM (right).

The superposition of an orthorectified image fragment of the optical base in the Google Earth viewer is shown in Fig. 8. The error in the XY-plane is about 2 m.

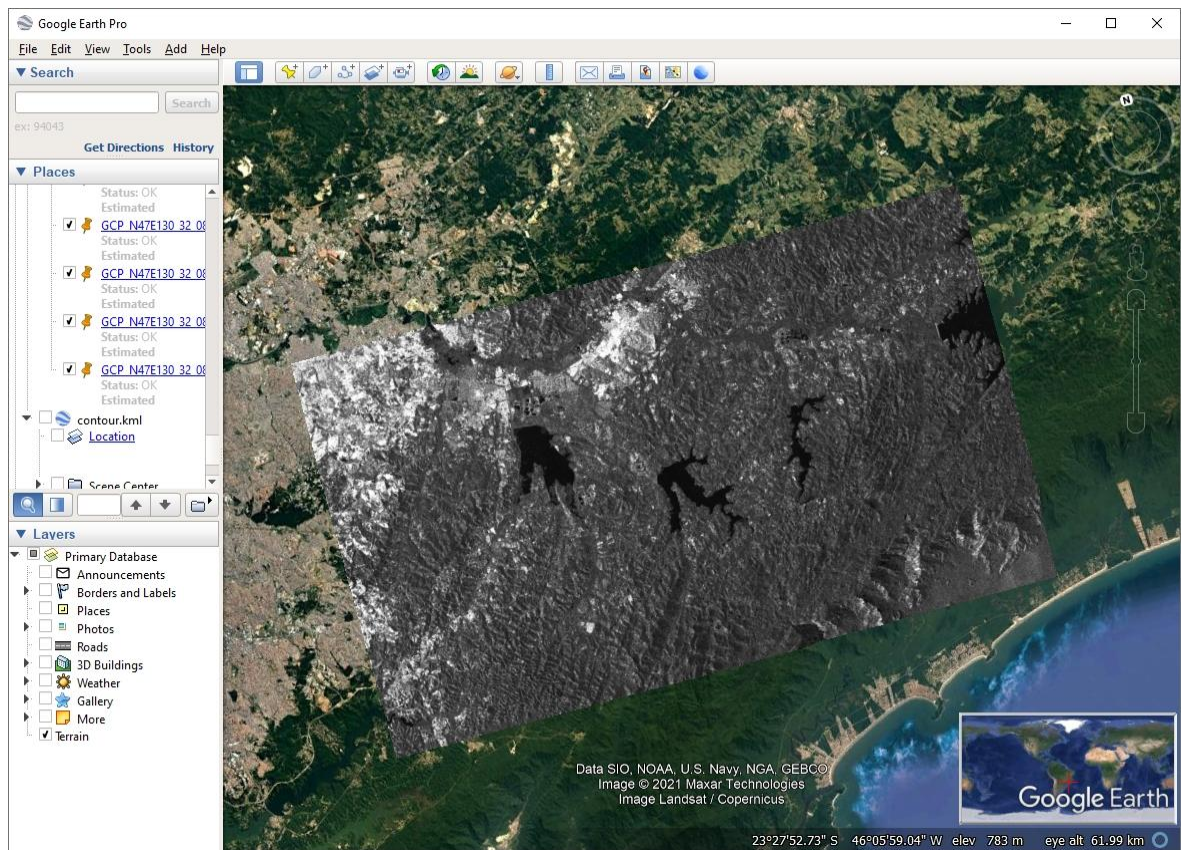


Fig. 8. A fragment of an orthorectified image in the Google Earth viewer

Creating a surface type digital map by the interferometric method

Initial data for the relevant processing example is a series of 5 multi-temporal complex SAR images obtained by Sentinel-1 (A, B) in June 2019 for the forested area in Amur Oblast north of the city of Blagoveshchensk.

Imaging dates were June 4, 2019; June 10, 2019; June 16, 2019; June 22, 2019; and June 28, 2019.

SLC product type, Stripmap mode, and VV VH polarization are involved.

The processing is performed in the “Interferometry” unit (“Coherent coregistration”).

After the input of pre-converted into the internal PHOTOMOD Radar format images, the images are matched with subpixel accuracy (each image is matched in sequence with the first one by the date of imaging).

Main operations (after coregistration, by the example of an enlarged image fragment) are illustrated below.

Numerical characteristics of image pixels over the whole series (mean amplitude, coefficient of amplitude stability, and mean coherence) are estimated.

Fig. 9 presents an image of the mean amplitude obtained through averaging over a series of images. This image has higher radiometric resolution than each single image of the series.



Fig. 9. Mean amplitude image

Fig. 10 presents an image of the coefficient of amplitude stability. Higher brightness values in this image (light areas) correspond to amplitude values slightly changing from one image to another. And vice versa, low brightness values (dark areas) correspond to unstable (changing) amplitude.

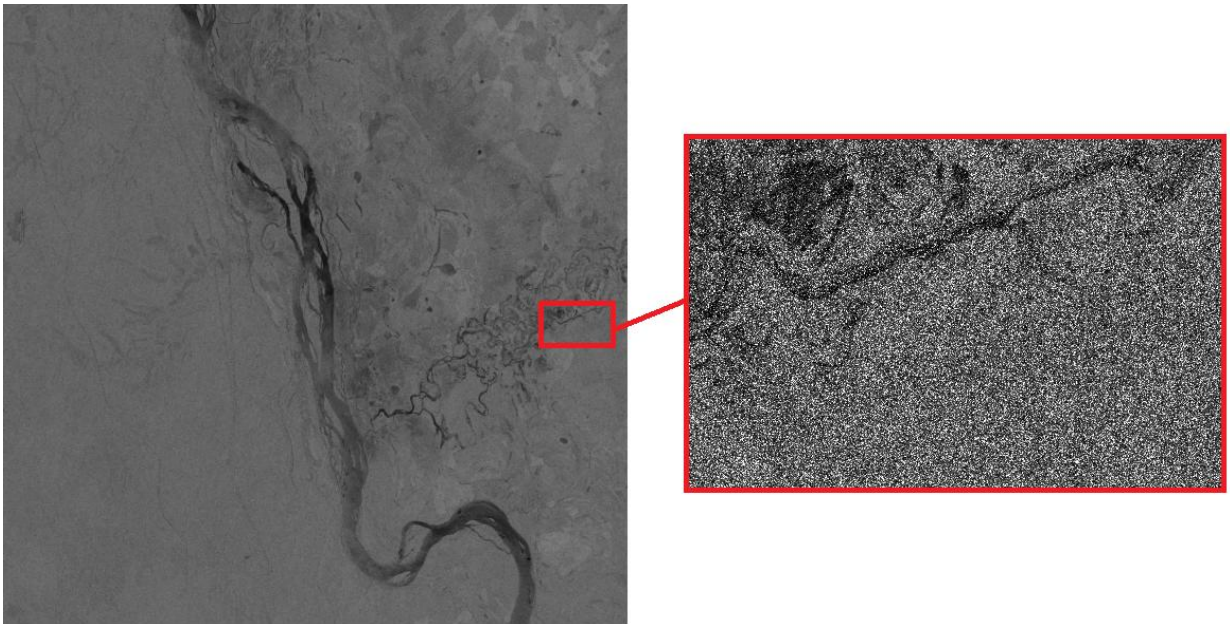


Fig. 10. Image of the coefficient of amplitude stability

An image of mean coherence is given in Fig. 11. High coherence values are typical for the areas with stable surface scattering properties (positions of single elementary reflectors inside SAR spatial resolution cell doesn't change between shootings). Low coherence values give evidence of temporal decorrelation due to surface scattering property fluctuations.

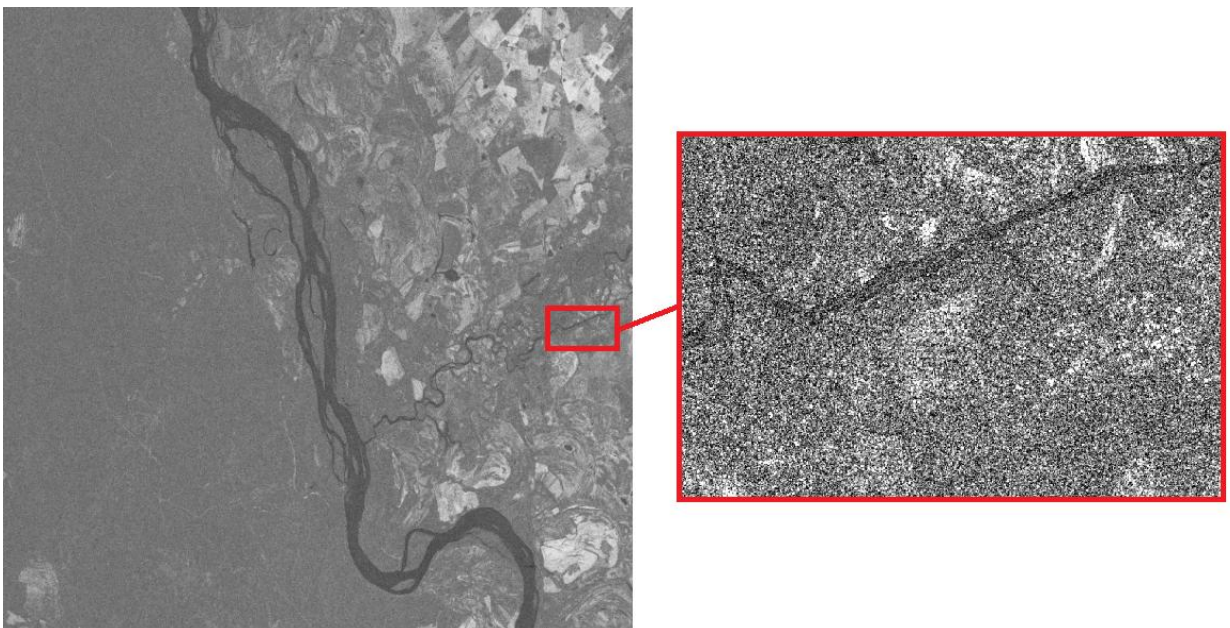


Fig. 11. Mean coherence image

At the stage of estimation of numerical characteristics, it is also possible to view a false color image that is a composition of calculated characteristics (Fig. 12). The red band is the amplitude stability, the green band is the mean amplitude, and the blue band is the mean coherence. Color of a pixel corresponds its numerical characteristics. For example, red color corresponds to stably low amplitude and low coherence what occurs in the area of the radar shadow:

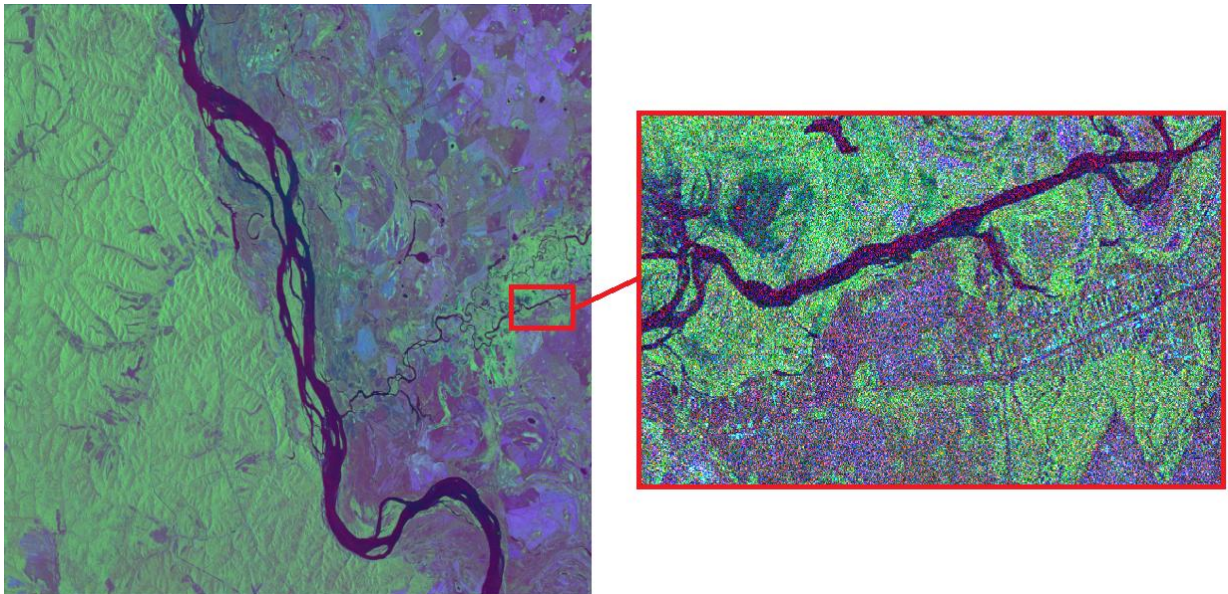


Fig. 12. Pseudocolor representation of the estimated pixel characteristics

At the next stage, a digital map of coherent change detection is being created that is an interim result of coherent coregistration of several radar images (Fig. 13).

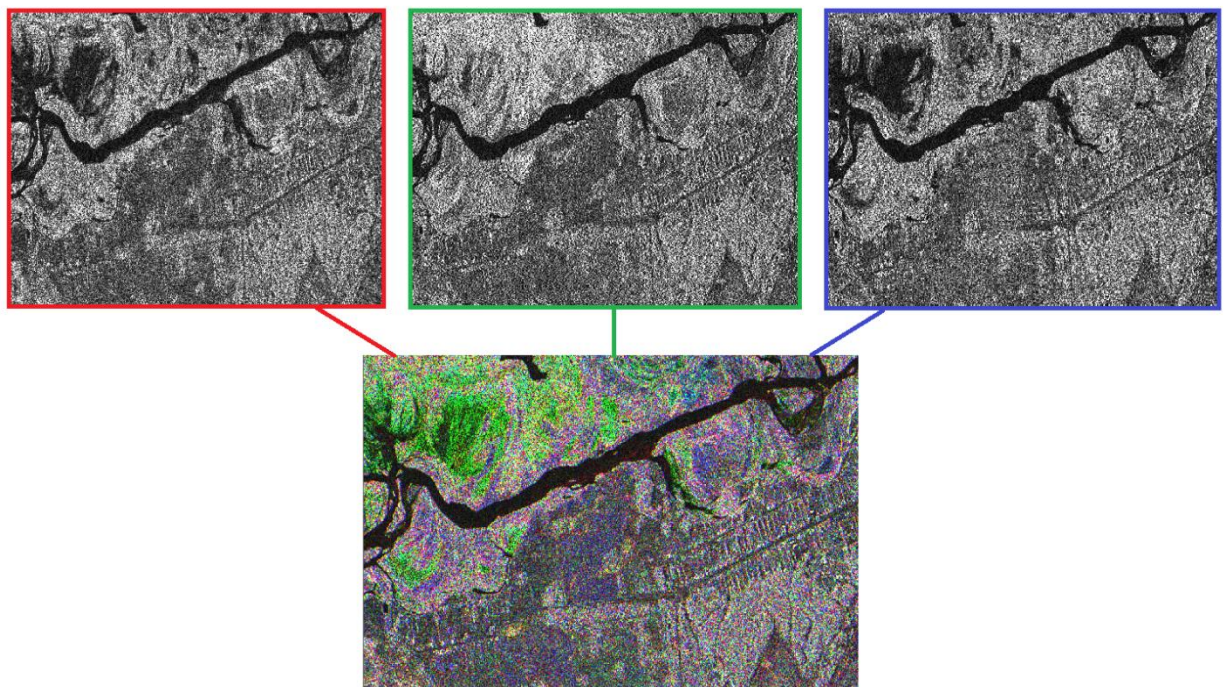


Fig. 13. A false color image representing the composition of three images (by amplitude)

The result of spatial coregistration of amplitude radar images is the digital map of amplitude change detection that is given in Fig. 14 as a composition of three image-differences.

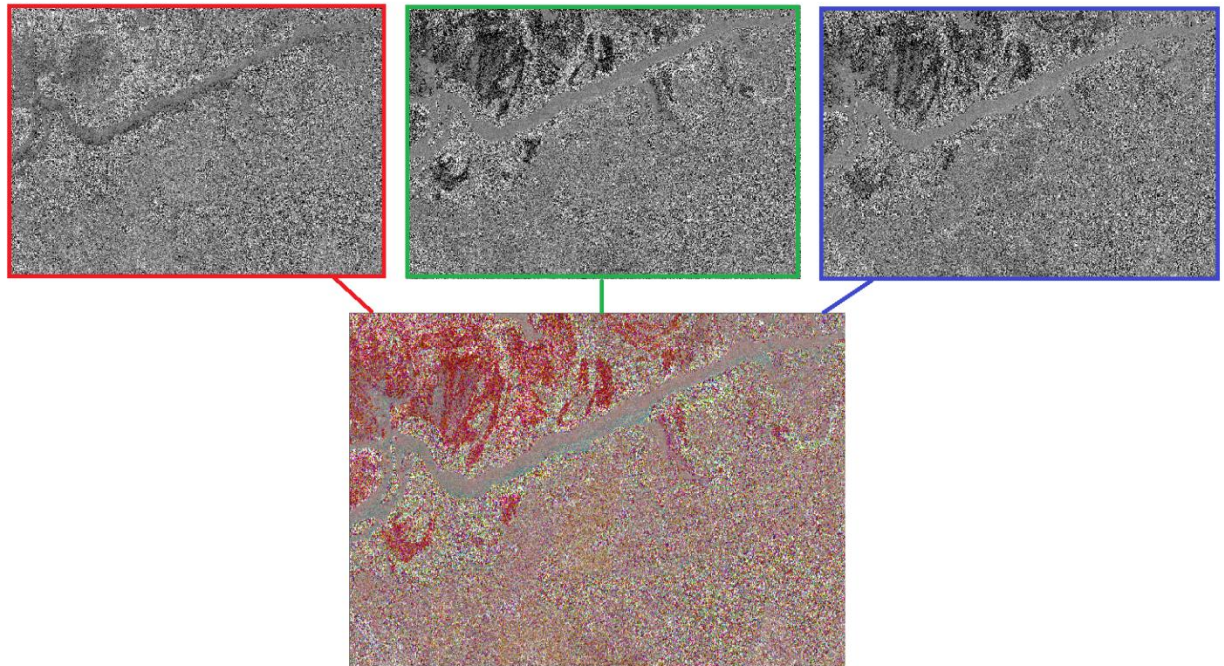


Fig. 14. False color representation of amplitude differences

The final processing step is a digital map of surface types (class matrices). Fig. 14 represents a matrix using numerical characteristics.

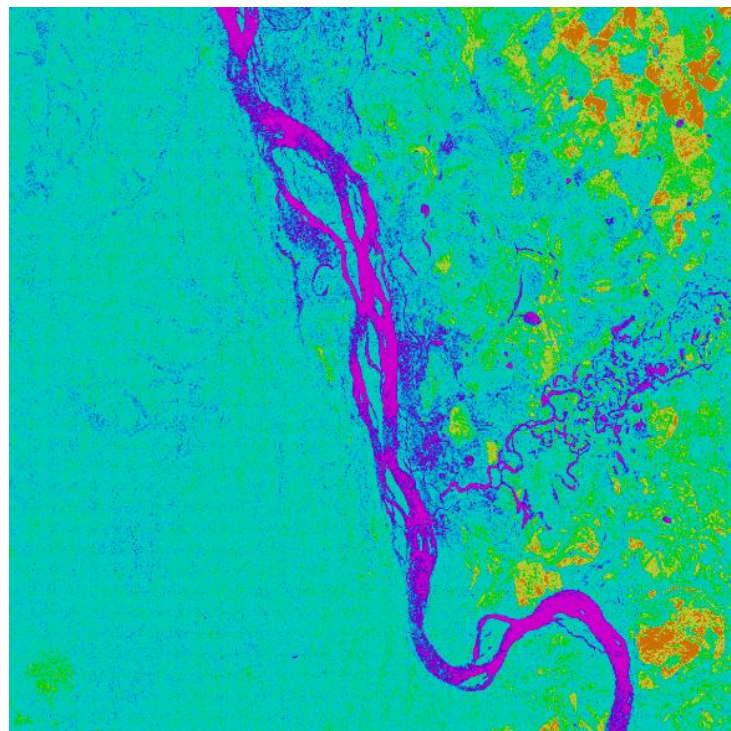


Fig. 15. Surface type digital map (classification result)

According to the results of preliminary interpretation, four classes prevail: blue and bright pink (water surface, radar shadow), blue (vegetation), green (deforestation), and yellow and brown (urban areas, agricultural land).

Thus, in particular, the series of images for the same surface region allows us to obtain a radar image with increased radar resolution and estimate the degree of variation of surface scattering properties from image to image that is illustrated in Fig. 16 by the example of an image fragment.

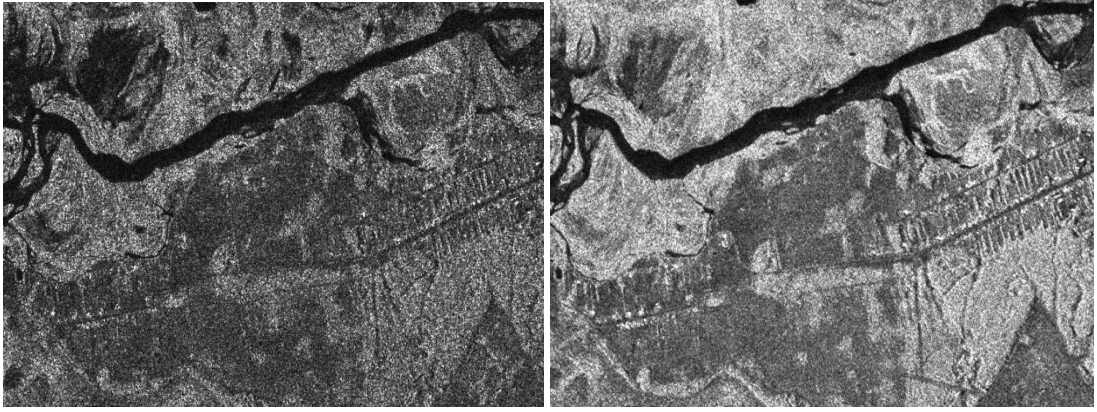


Fig. 16. Comparison of original June 4, 2019 image fragment (left) and mean amplitude image (right)

Detecting surface vessels and estimating their characteristics

The processing is performed in “Marine applications” unit (“Ships”).

Initial data is the amplitude marine surface SAR image containing ship images obtained by Sentinel-1A on February 11, 2020 for the water area region in the Strait of Gibraltar.

GRD product type, Interferometric Wide swath (IW) mode, and VV polarization are involved.

After preliminary converting into the internal PHOTOMOD Radar format, an image fragment shown in Fig. 17 is selected for further processing.

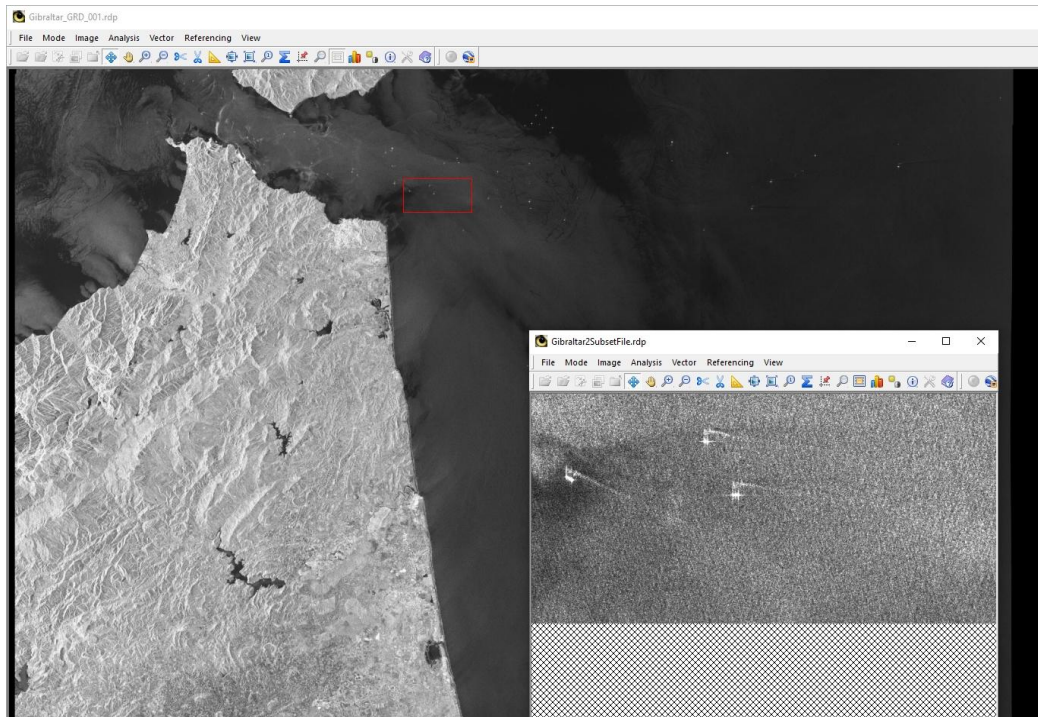
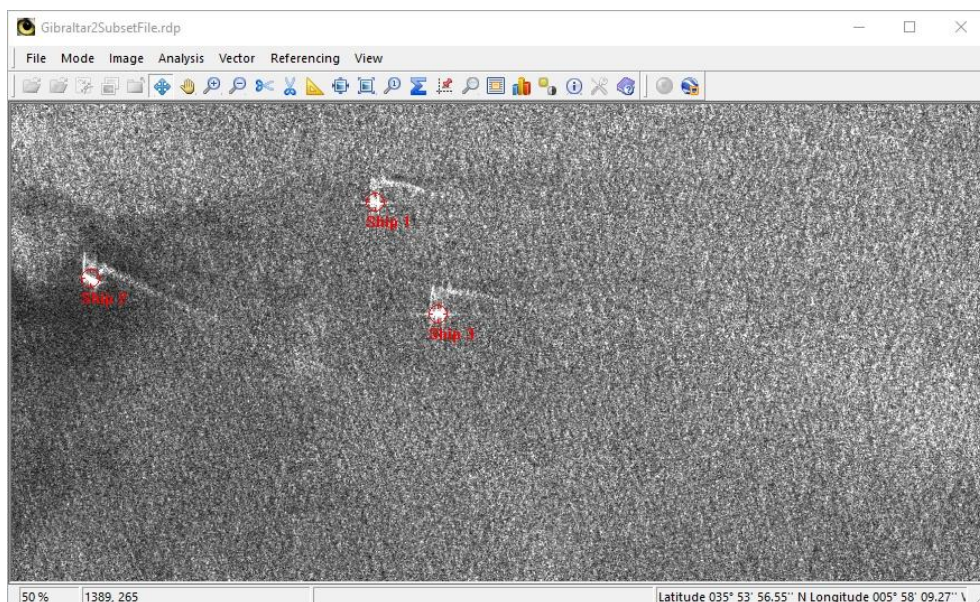


Fig. 17. A SAR fragment displaying ships for the processing

Main stages of the selected image fragment processing are illustrated below.

The search for ships is carried out in automatic mode. Herewith, the program produces the list of detected ships and determines their geographic coordinates (Fig. 18).



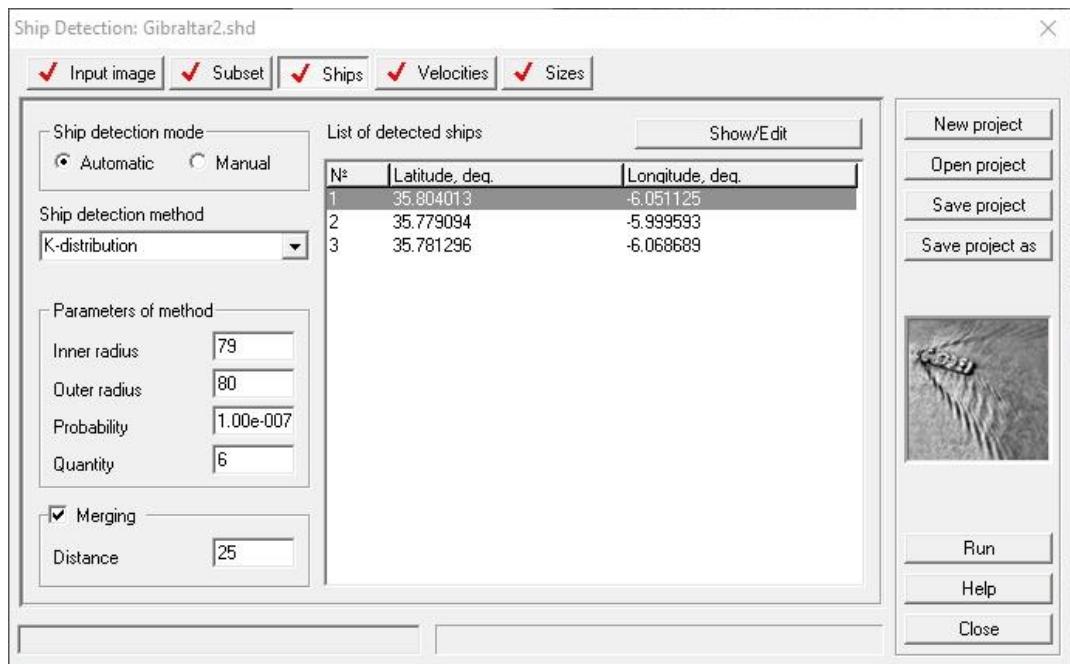
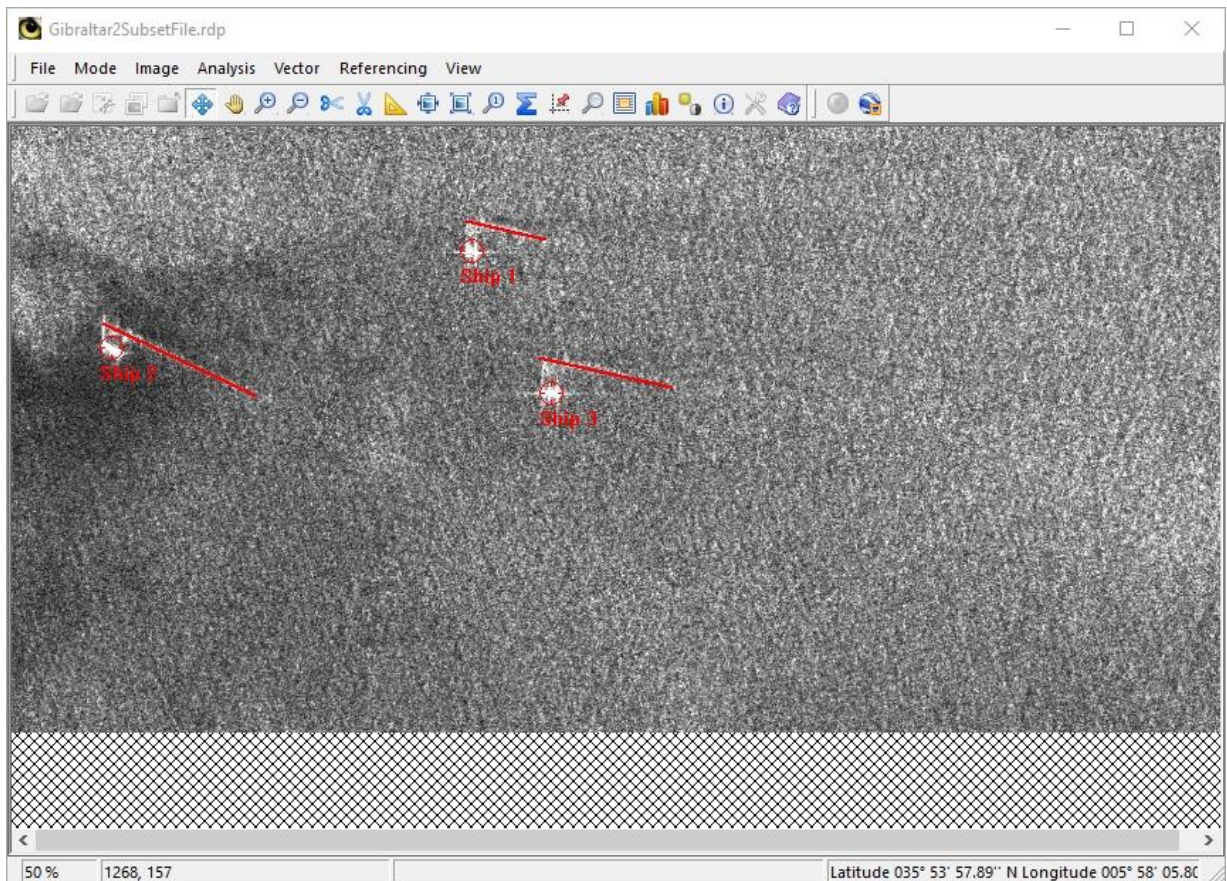


Fig. 18. The tab after ship search in automatic mode (bottom), and the viewer (top).

The program also allows for ship's speed estimation. For this, beforehand it is required to select manually wakes as it is shown in Fig. 19.



List of ships

Nº	Name	Color	Col	Row	Req col	Req row	End col	End row
1	Ship 1		646.000	174.000	637.000	132.000	748.000	158.000
2	Ship 2		139.000	310.000	128.000	275.000	343.000	377.000
3	Ship 3		757.000	372.000	740.000	323.000	927.000	365.000

Load Save Close


Ship Detection: Gibraltar2.shd

Input image Subset Ships Velocities Sizes

Absolute ship velocities Show/Edit

Nº	Latitude, deg.	Longitude, deg.	Velocity, knots.	Azimuth, deg.
1	35.804013	-6.051125	11.741518	82.994004
2	35.779094	-5.999593	9.945429	68.489189
3	35.781296	-6.068689	13.267136	82.989442

New project
Open project
Save project
Save project as



Run
Help
Close

Fig. 19. The tab after speed estimation (bottom), the viewer with manually selected wake (top).

The final processing step is the determination of ship sizes. This task is solved in automatic mode. The appearance of the tab after size determination operation is shown in Fig. 20.

Ship Detection: Gibraltar2.shd

Input image Subset Ships Velocities Sizes

Report of results Show/Edit

Nº	Latitude, deg.	Longitude, deg.	Velocity, knots.	Azimuth, deg.	Length, m.	Width, m.
1	35.804013	-6.051125	11.741518	82.994004	191.049732	60.827625
2	35.779094	-5.999593	9.945429	68.489189	322.490310	89.442719
3	35.781296	-6.068689	13.267136	82.989442	280.178515	140.356688


Calculation mode: Automatic Manual

Output files:

File *.txt: \\HEAP1\kspo\0... лей_Гибралтар\Gibraltar2Result.txt

File *.shp: \\HEAP1\kspo\0... лей_Гибралтар\Gibraltar2Result.shp

New project
Open project
Save project
Save project as



Run
Help
Close

Fig. 20. The tap appearance after ship size determination

The result of the program execution is a text file that contains the list of detected surface vessels and the data on their geographic position, speed, azimuth, and linear size (Fig. 21).

```
RESULTS OF PROCESSING

Coordinates of scene corners
-----
| Corner      | Latitude, deg. | Longitude, deg. |
-----
| Left up     | 35.899         | -5.959          |
| Right up    | 35.926         | -6.146          |
| Left bottom | 35.822         | -5.976          |
| Right bottom| 35.849         | -6.163          |
-----

Time of survey

Year    2020
Month   2
Day     11
Hour    6
Minute  27
Secunde 47

List of detected ships
-----
| № | Latitude, deg. | Longitude, deg. | Velocity, knots. | Azimuth, deg. | Length, m. | Width, m. |
-----
| 1 | 35.804         | -6.051          | 11.742           | 82.994        | 191        | 60        |
| 2 | 35.779         | -6.000          | 9.945            | 68.489        | 322        | 89        |
| 3 | 35.781         | -6.069          | 13.267           | 82.989        | 280        | 140       |
-----
```

Fig. 21. Text file of the report on the processing carried out in the ship detection unit

Detecting oil slicks in radar imagery

The processing is carried out in the “Marine applications” unit (“Oil slicks”).

A Sentinel-1A image of October 14, 2018 for the region of water area near Corsica is used in the example given below. GRD product type, Interferometric Wide swath (IW) mode, and VV polarization are involved.

After preliminary converting into the internal PHOTOMOD Radar format, an image fragment shown in Fig. 22 is selected for further processing.

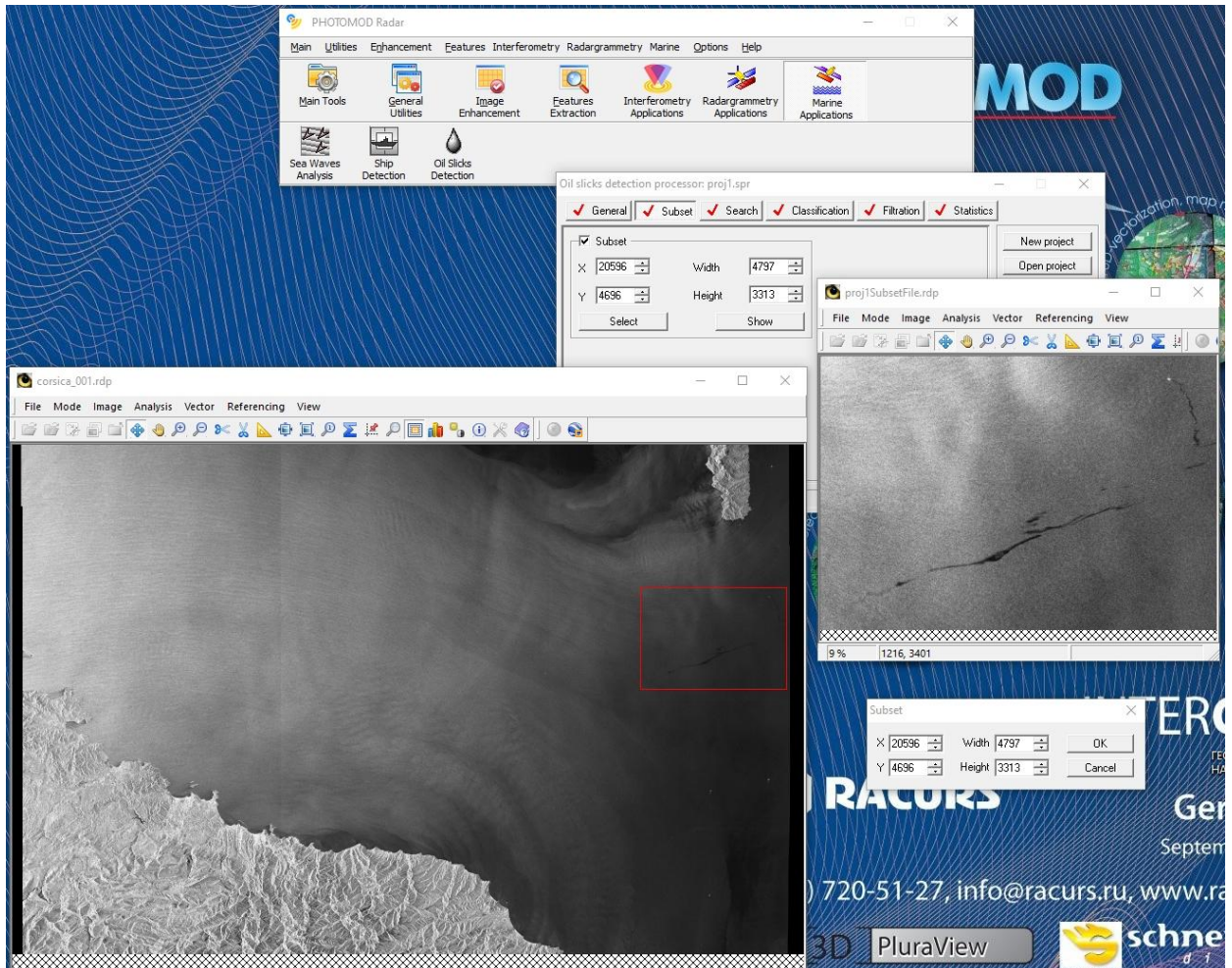


Fig. 22. A radar image fragment for the processing displaying an oil slick on the uniform sea surface. Main stages of the selected image fragment processing are illustrated below.

The initial sorting of input image elements is performed for subsequent iterative classification. Fig. 23 shows the result of oil slick search in radar imagery.

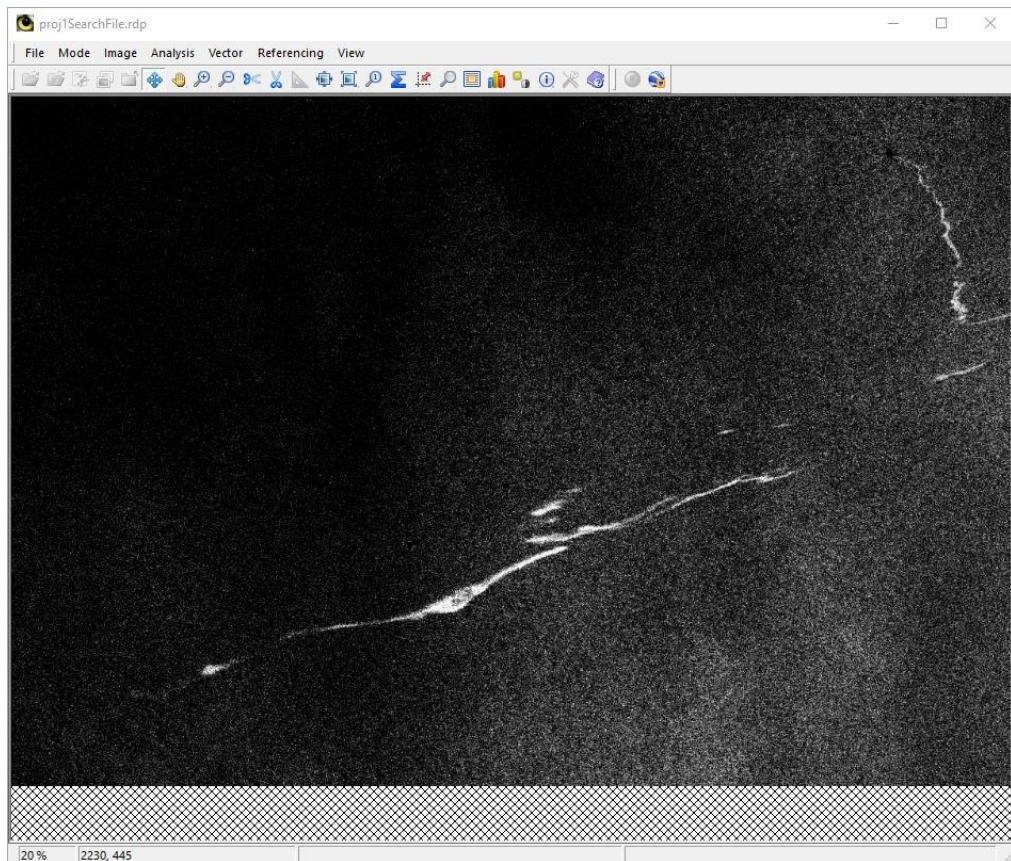


Fig. 23. The result of oil slick search in radar imagery

Next, the classification is carried out when the pixels of the processed area of the image are sorted into two classes. The classification result is shown in Fig. 24.

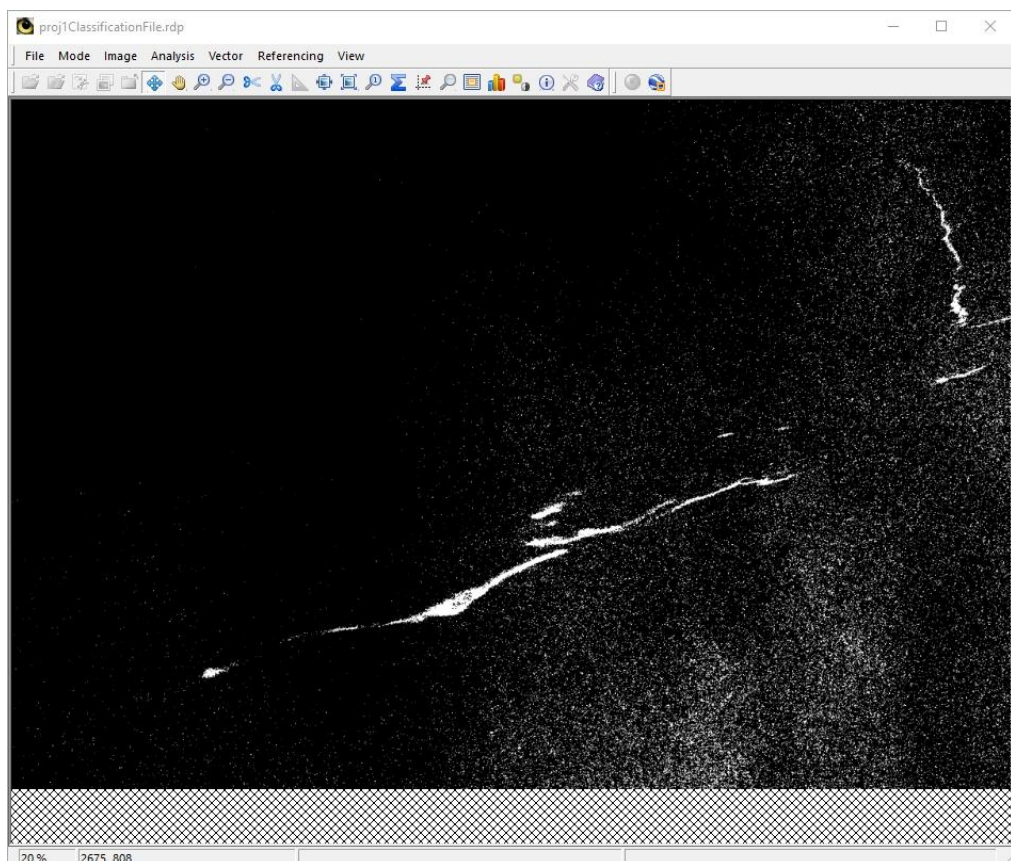


Fig. 24. Classification result

To increase spatial homogeneity of the classification result, it is feasible to perform filtering. The filtering result is shown in Fig. 25.

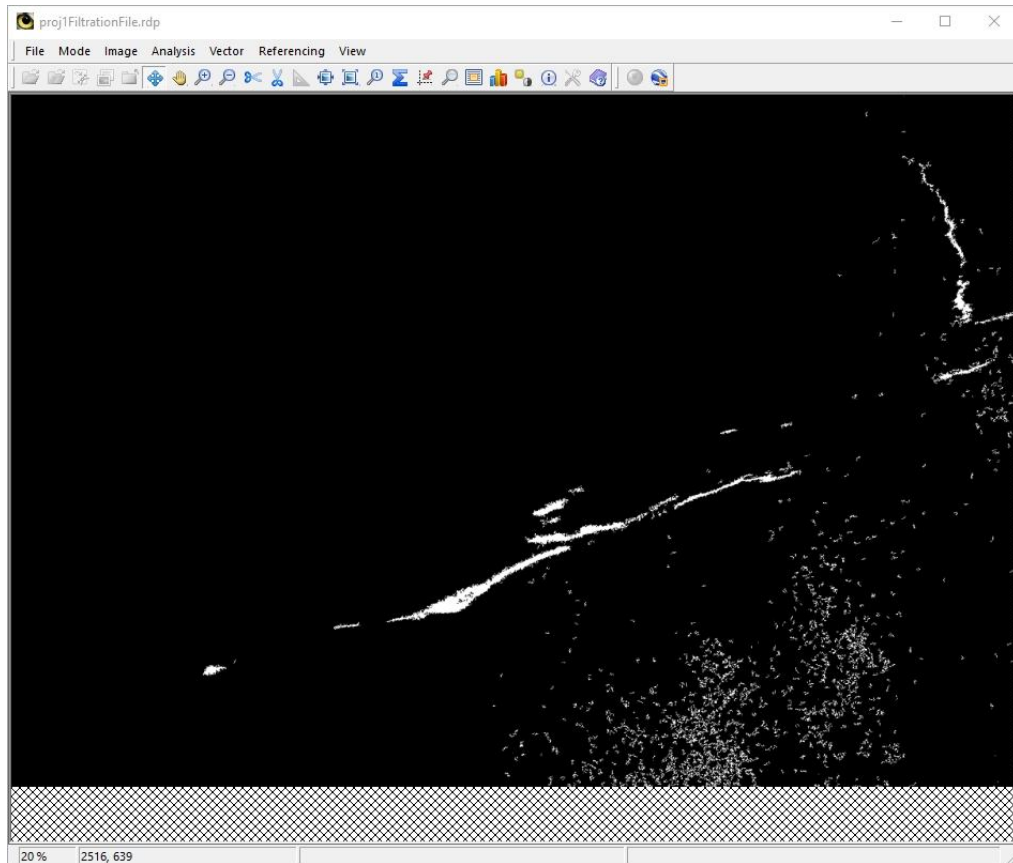
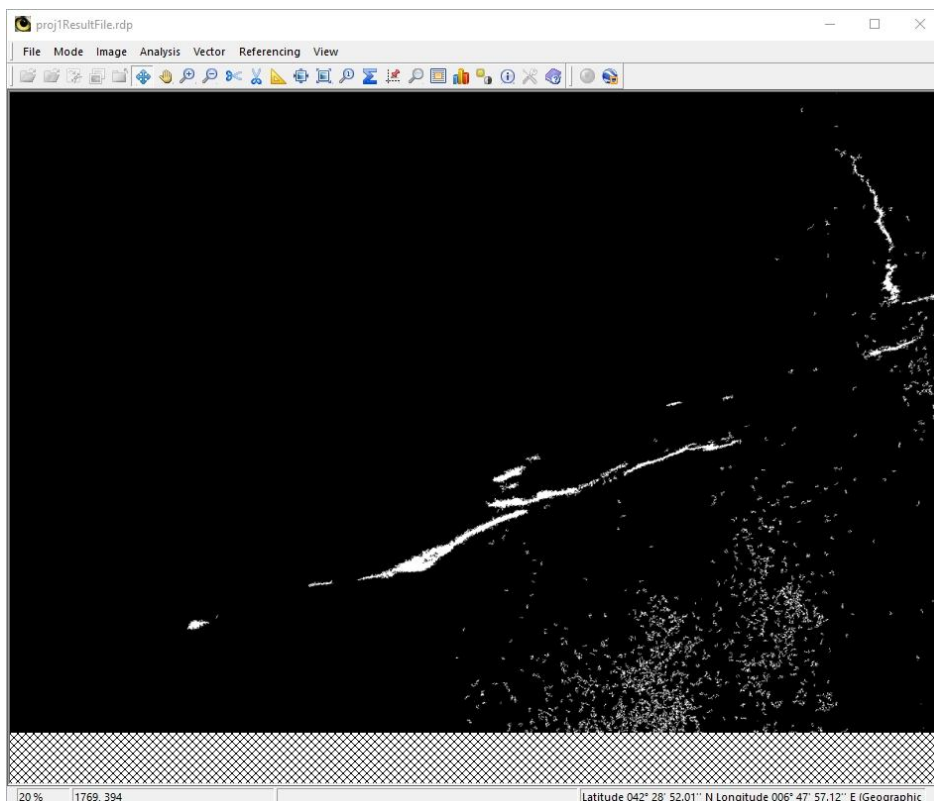


Fig. 25. Filtering result

At the final stage, total area of detected oil slicks in the selected radar image fragment is determined (Fig. 26).



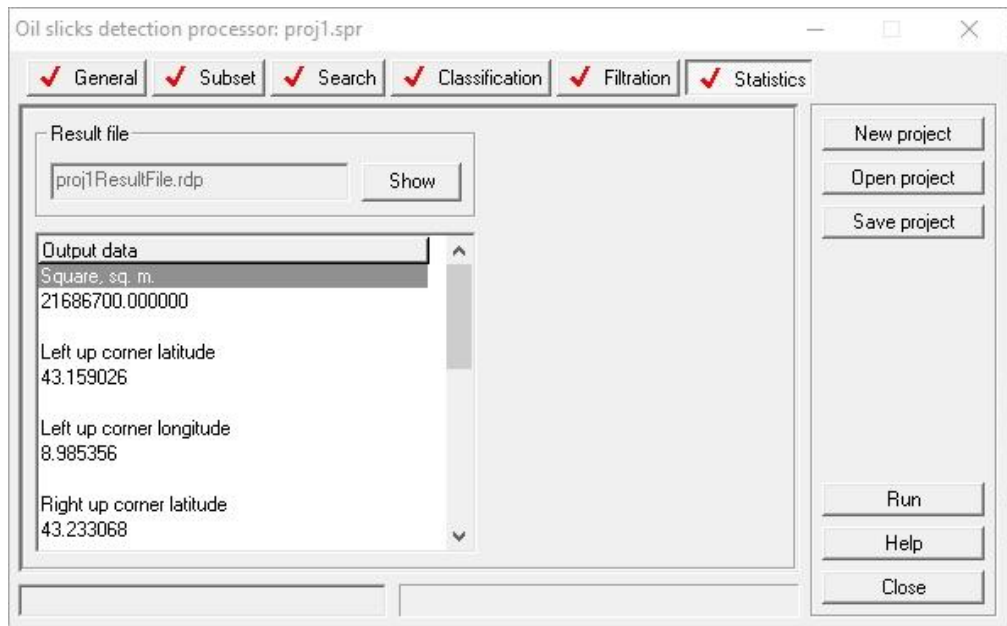


Fig. 26. The tap after the calculation of statistics by a radar image (bottom), and the viewer (top)

Analyzing sea waves in radar imagery

The processing is carried out in the “Marine applications” unit (“Sea waves”).

As the initial data, a radar image of the sea surface is selected, displaying well defined wave structure. A Sentinel-1A image of April 27, 2015 for a region of the water area near San Diego, California. GRD product type, Stripmap mode, and VV polarization are involved.

After preliminary converting into the internal PHOTOMOD Radar format, an image fragment shown in Fig. 27 is selected for further processing. Large energy-carrying waves on the sea surface are clearly displayed in the image fragment.

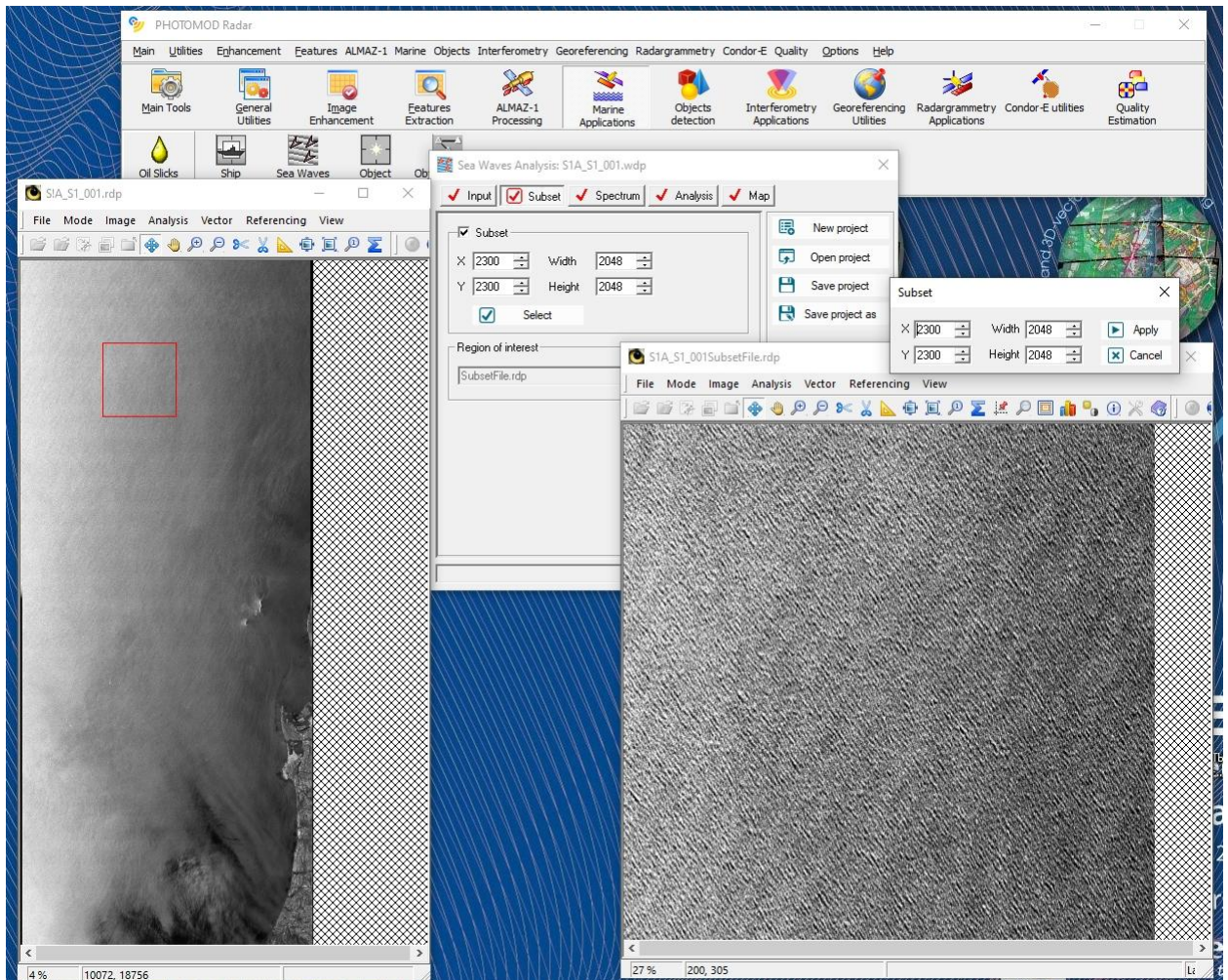


Fig. 27. A radar image fragment for the processing showing well defined wave structure

Main stages of the selected image fragment processing are illustrated below. The 2D spectrum of the selected image fragment is calculated as it is shown in Fig. 28.

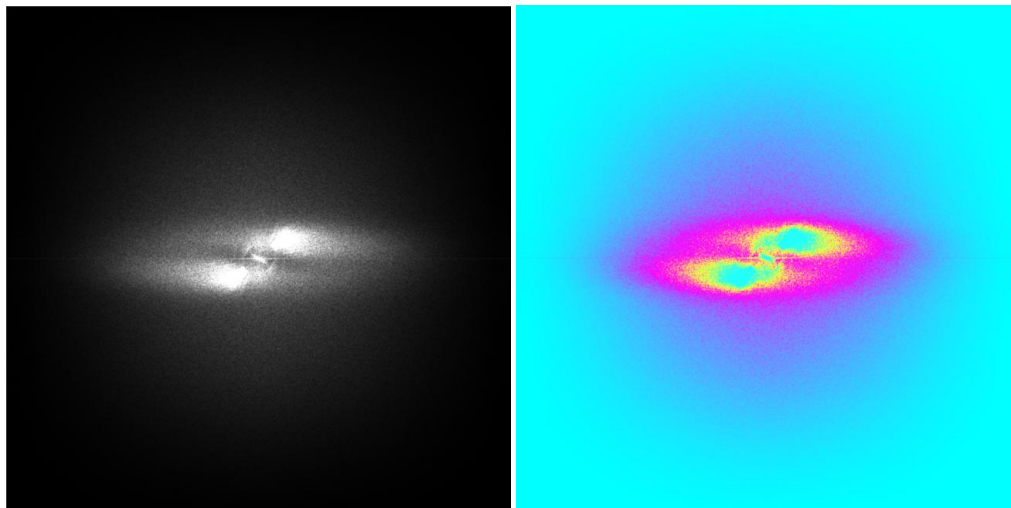


Fig. 28. Grayscale (left) and false color (right) spectrum calculation results

The spectrum analysis is further performed. The text file generated at this stage contains the average characteristics of sea waves, reduced to the center of the scene, geographical coordinates of the scene of interest, and the date/time of the scene center imaging (Fig. 29).

PHOTOMOD Radar

Main Utilities Enhancement Features ALMAZ-1 Marine Objects Interferometry Georeferencing Radargrammetry Condor-E Quality Options Help

Main Tools General Utilities Image Enhancement Features Extraction ALMAZ-1 Processing Marine Applications Objects detection Interferometry Applications Georeferencing Utilities Radargrammetry Applications Condor-E utilities Quality Estimation

Oil Slicks Detection Ship Detection Sea Waves Analysis Object Detection Object Motion

Sea Waves Analysis: S1A_S1_001.wdp

Input Subset Spectrum Analysis Map

Parameters of detected waves

Parameter	Value
Wave Direction, deg	115.126833
Wave Space Period, m	143.261117
Wave Height, m	3.581528
Wind Velocity, m/sec	13.118214
Survey date, dd.mm.yy	27.04.2015
Survey time, hh:mm:ss	01:41:10.785777

Processing parameters

Deep-water Shallow-water

Depth, m: 10.000000

Radius of excluded area, pixels: 30

File of results: \\NEAP1\ksp\Морское во... го_новый проект - Сору\ \\NEAP1\ksp\Морское волнение_Сан-Диего_н

RESULTS OF PROCESSING

Coordinates of scene corners

Corner	Latitude, deg.	Longitude, deg.
Left up	31.674	-117.546
Right up	31.710	-117.332
Left bottom	31.857	-117.590
Right bottom	31.894	-117.377

Time of survey

Year: 2015
Month: 4
Day: 27
Hour: 1
Minute: 41
Secunde: 10

Wave parameters

Wave direction, deg: 115.126833
Wave space period, m: 143.261117
Wave height, m: 3.581528
Wind velocity, m/sec: 13.118214

Fig. 29. The tab after the spectrum analysis indicating calculated characteristics of detected waves

Apart from the text file, the processing results are the created maps of spatial distribution of sea wave characteristics (Fig. 30). At this stage, spatial distribution of wind speeds in m/s (top left) and spatial distribution of wind directions in deg (top right) are performed automatically. Also, maps are built that allow us to estimate large wave elevations in meters (bottom left) and their spatial period in meters (bottom right).

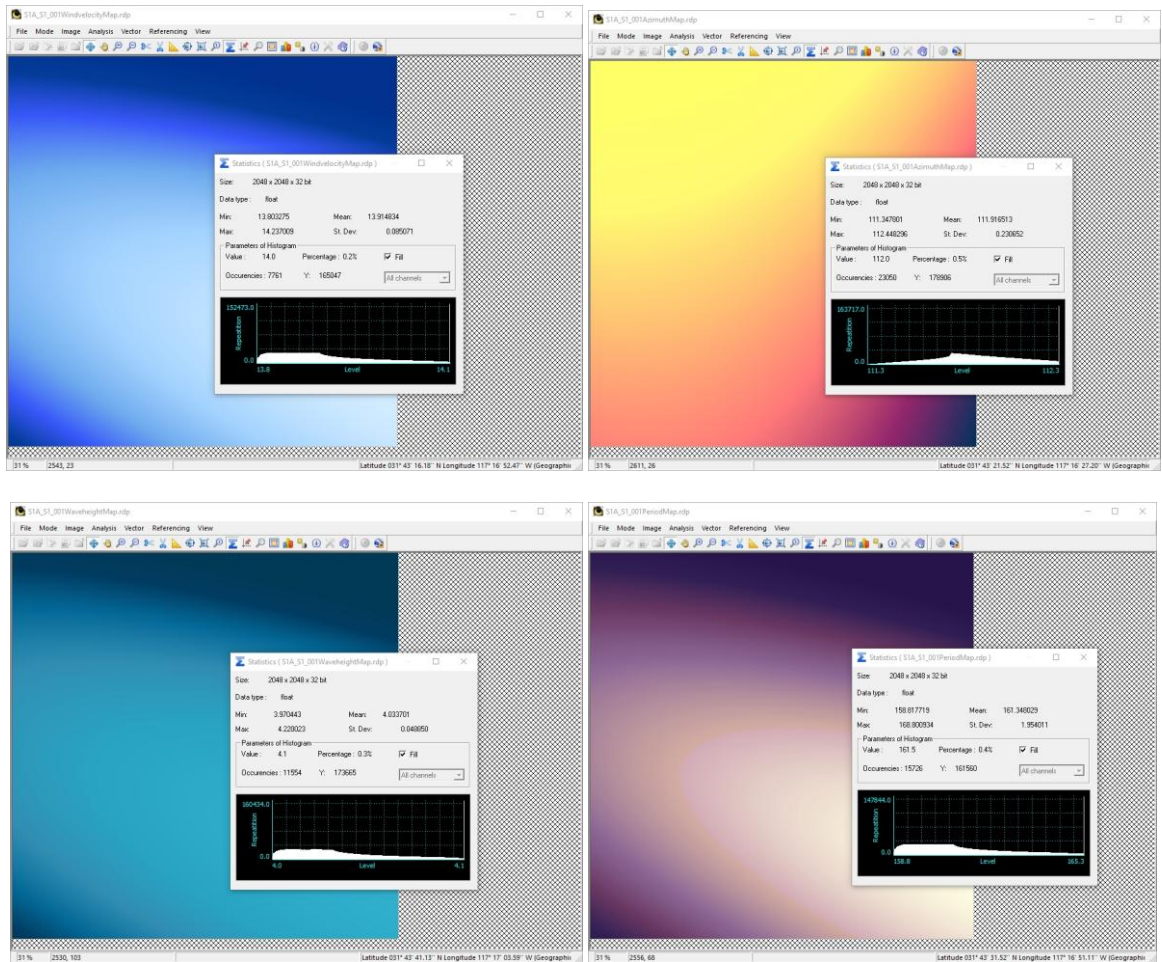


Fig. 30. Spatial distribution of sea wave characteristics

Orthorectifying of radar imagery

The example given below is the Sentinel-1 image for the region in Volgograd Oblast. The product ID is S1A_IW_GRDH_1SDV_20150525T031358_20150525T031423_006072_007DB8_604E.SAFE.

One coaxial VV and one cross VH polarization images are included in the product. The coaxial polarization image s1a-iw-grd-vv-20150525t031358-20150525t031423-006072-007db8-001.tiff was processed.

The analysis was carried out using PHOTOMOD Radar, Google Earth Pro, and Global Mapper v12.02 software. The processing in PHOTOMOD Radar software was carried out using a geocoding processor.

Figures 31 and 32 show the imagery downloaded into Global Mapper and Google Earth viewers.

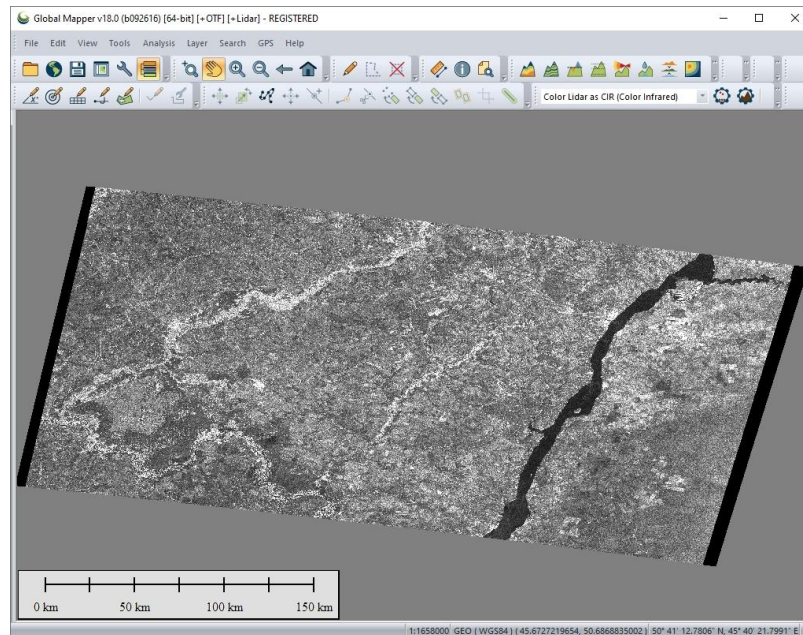


Fig. 31. An image downloaded into Global Mapper

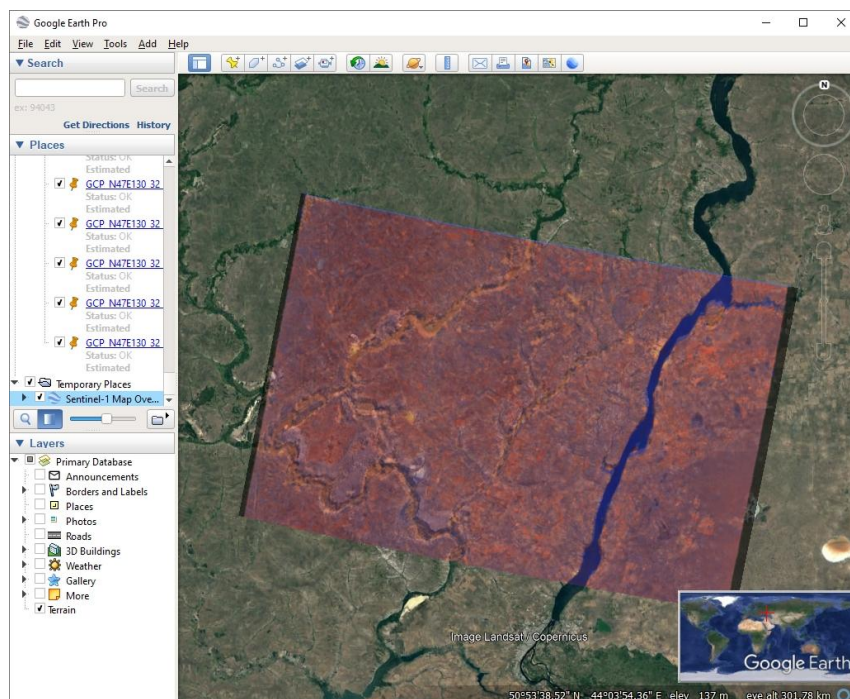


Fig. 32. An image downloaded into Google Earth

Since both programs let the user to obtain geographic coordinates of any image pixel, measurements of coordinates of identical points in both programs were carried out. These measurements have shown that the difference between the positions of points in the radar image in Global Mapper and those in optical basemap in Google Earth is 70 – 90 meters.

It is to be noted, that the accuracy of such measurements are limited by the radar image resolution that is more than 20 meters for both coordinates. Capabilities of practical evaluation of referencing Sentinel-1 data of this format are illustrated in Figures 33 and 34, where enlarged fragments of the same surface region in Global Mapper and Google Earth are shown. As we can see from these figures, the search of identical points in Sentinel-1 images can be made with an error of several (1-3) pixels, that causes two or three tens of meters error of reference evaluation.

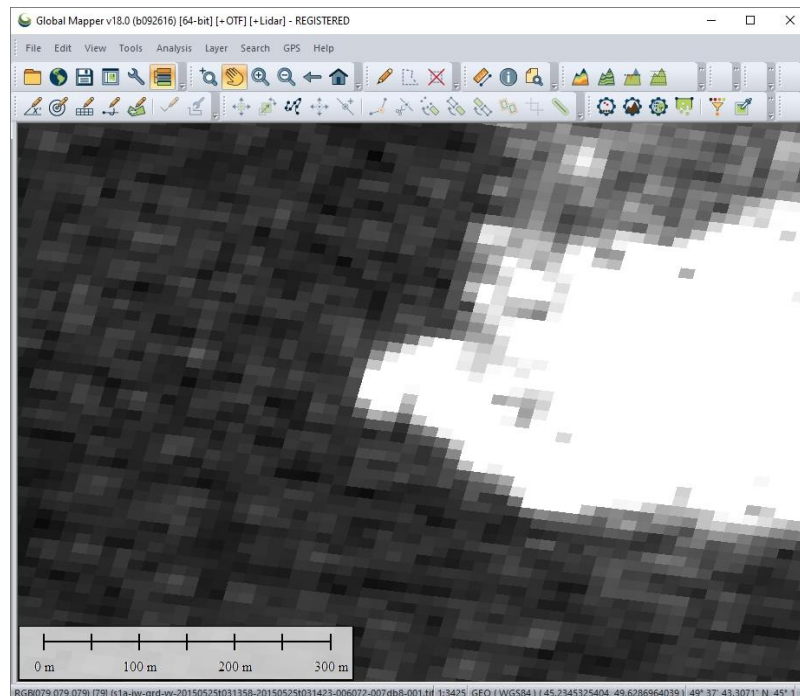


Fig. 33. A fragment of sea surface region in the Global Mapper viewer

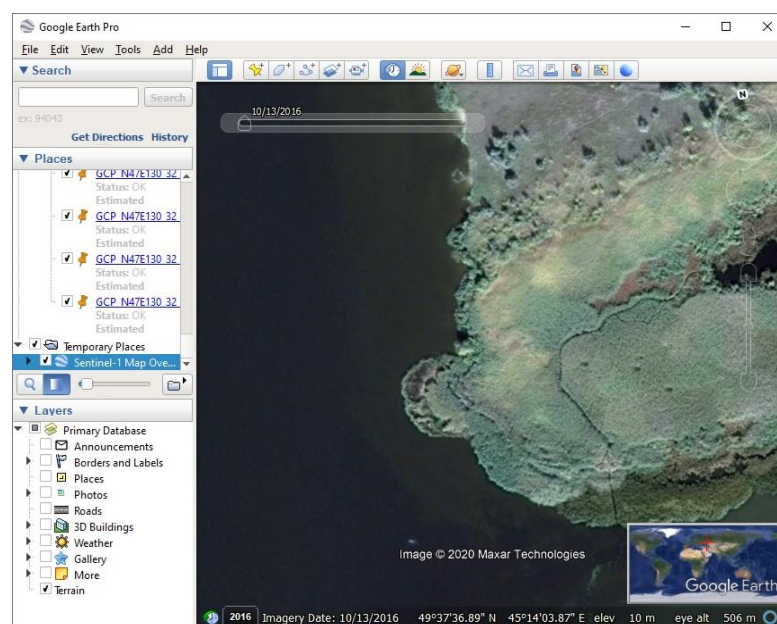


Fig. 34. A fragment of sea surface region in the Google Earth viewer

For the quality assessment of scene service information used during radargrammetric transforms, the orthorectification of a Sentinel-1 image in the PHOTOMOD Radar package geocoding processor was performed. The orthorectification was carried out using a strict model on an altitude-longitude grid according to the parameters of the service information of the scene using data on the terrain from the global SRTM 3.1 DEM. Elevation data were downloaded automatically without preliminary creation of control terrain raster. Initial conditions (spacecraft state vectors and velocity at the survey moment) were not clarified. The orthorectification result is given in Fig. 35.

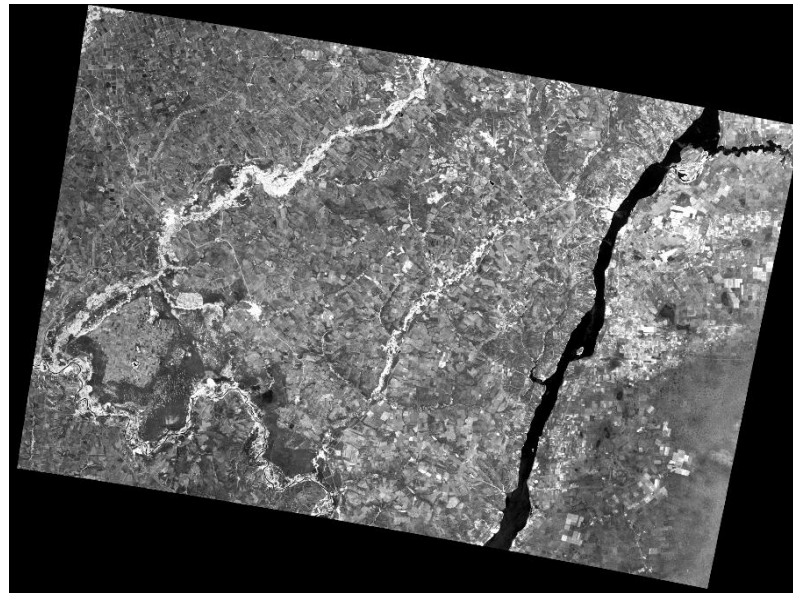


Fig. 35. Sentinel-1 orthorectified scene

To estimate service information parameter quality, we have compared the coordinates of points in the orthorectified image and in the Google Earth viewer. The positions of points differed by 20-60 meters. Decreased discrepancy in reference to the initial image may be caused by terrain displacement correction in the orthorectified image.

Fig. 36 shows the superposition of the orthorectified image on the optical basemap in the Google Earth viewer.

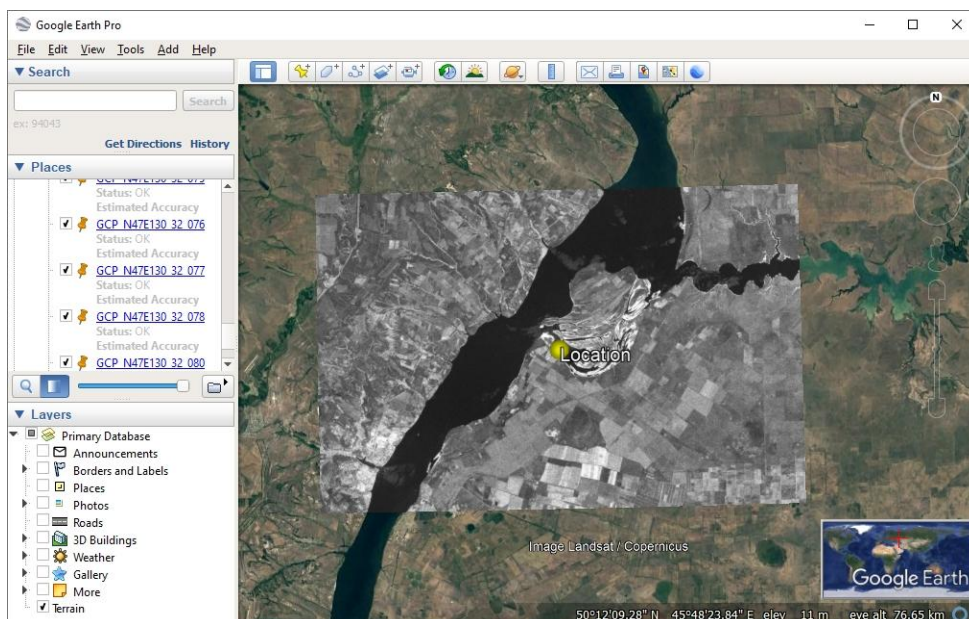


Fig. 36. The orthorectified image in the Google Earth viewer

Additional accuracy estimation for the referencing of the Sentinel-1 image orthorectified using service information was carried out using TM Landsat global coverage with 30 m pixel size. For the orthorectified radar image, a Landsat optical basemap with raster dimensions and interpixel distance identical to this radar image was created using the image coregistration program from the PHOTOMOD Radar software. Data sampling from the global coverage and optical raster creation were completely automatic. The information on radar raster and optical basemap pixel coordinates was only used, without the correlation analysis or any manual matching.

The accuracy of radar and optical rasters is about 30 - 70 meters.

The results of image coregistration in the PHOTOMOD Radar viewer in the “shatter” mode are shown in Figures 37 and 38 for the whole scene and a separate fragment, respectively.

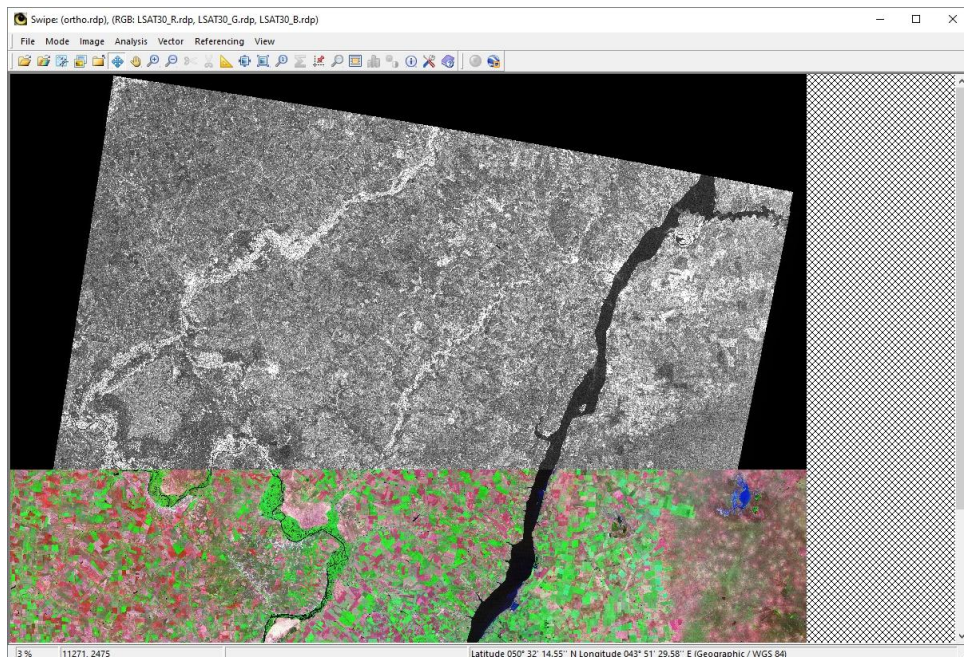


Fig. 37. Coregistrating radar and optical rasters

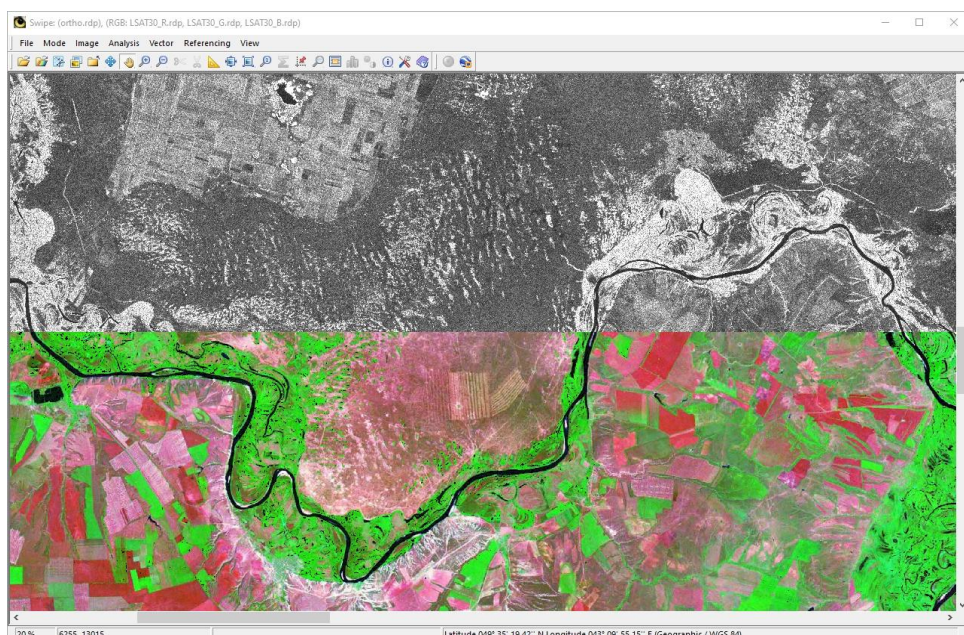


Fig. 38. Coregistrating radar and optical rasters (fragment)

Figures 39, 40, and 41 present the results of an artificial image creation that is synthesized using Sentinel-1 and TM Landsat data. Fig. 39 presents a fragment of a raster from TM Landsat global coverage, Fig. 40 presents a fragment of a Sentinel-1 raster orthorectified using service information, and Fig. 41 presents a synthesized radar and optical image.

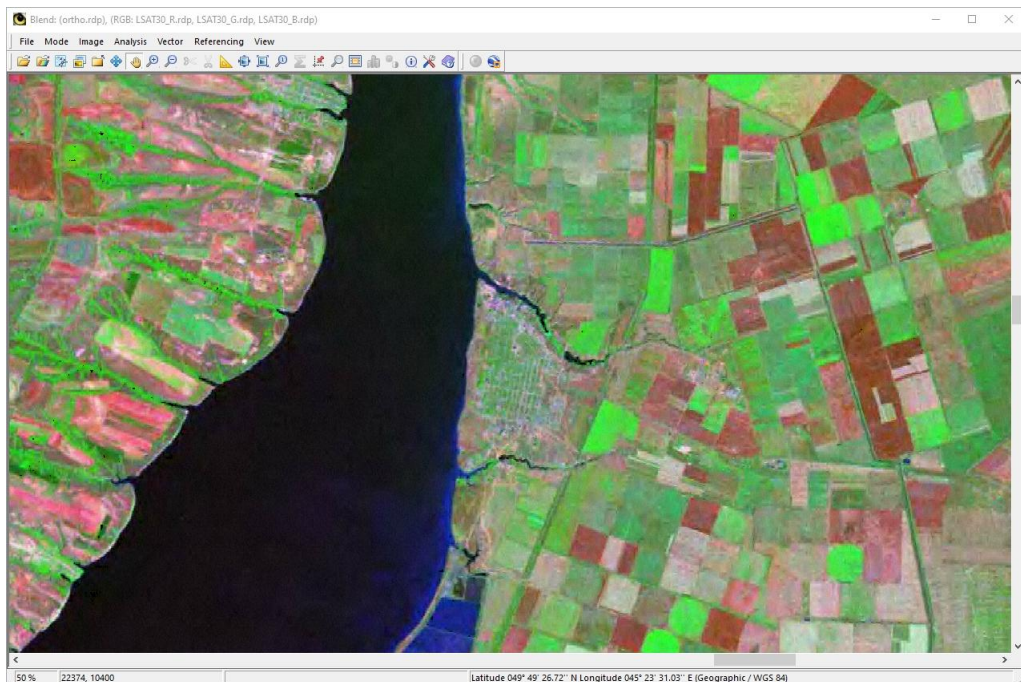


Fig. 39. TM Landsat optical global coverage fragment

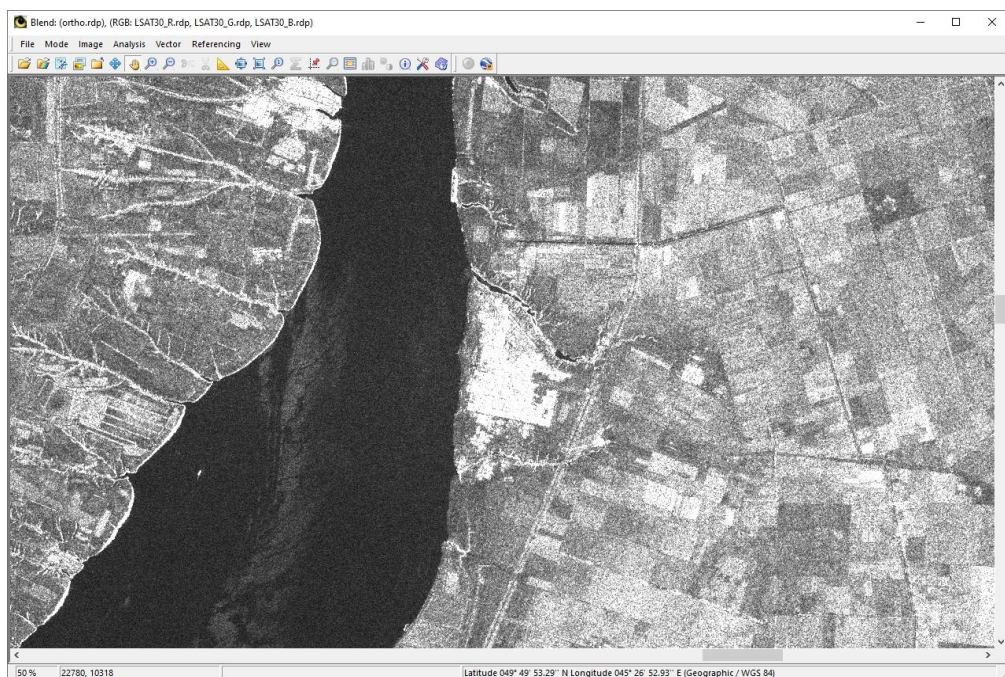


Fig. 40. Sentinel-1 orthorectified image fragment

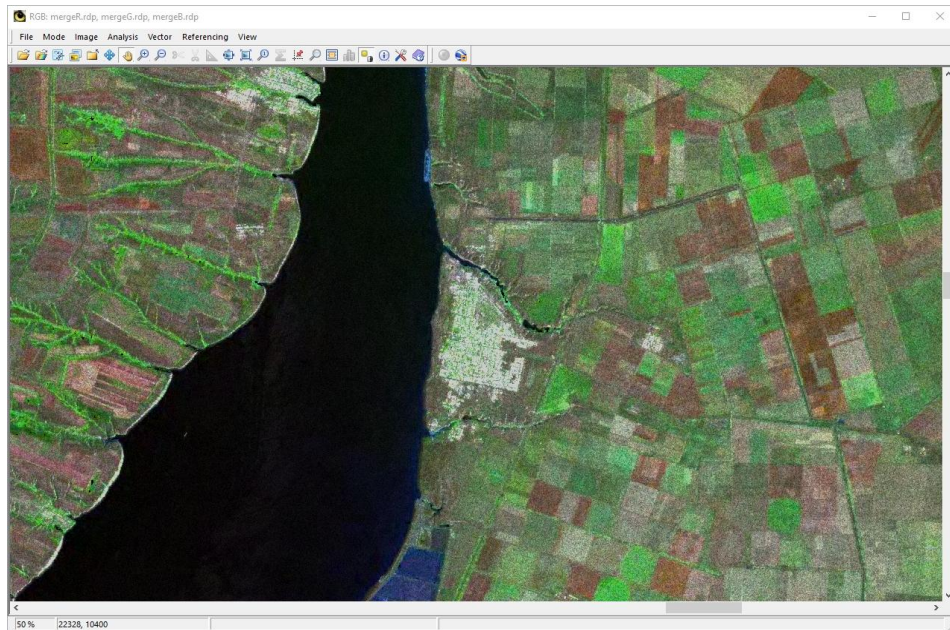


Fig. 41. Synthesized radar optical image.

The following concepts, abbreviations and terms are used in this document:

SAR – synthetic aperture radar;

SLC – single look complex. SLC products are in antenna coordinate SAR system or ACS (slant range - azimuth)

GRDH – ground range detected high resolution. GRDH products are in ground reference coordinate system or GFS (ground range - azimuth)